Research Square

Preprints are preliminary reports that have not undergone peer review.
They should not be considered conclusive, used to inform clinical practice,
or referenced by the media as validated information.

Aperture dilatation in DJAMILAR: Noether charge, localization drift, and a fixed-scale obstruction

ANISSE ZEROUTA

a.zerouta@precogtec.com

Precog Technologies– Theoretical Physics Division https://orcid.org/0000-0001-7966-0746

Research Article

Keywords: Djamilars, aperture dilatation, shift symmetry, Noether charge, ghost condensation, spontaneous localization, aether–scalar–tensor theory

Posted Date: September 30th, 2026

DOI: https://doi.org/10.21203/rs.3.rs-11206446/v1

License: This work is licensed under a Creative Commons Attribution 4.0 International License.
Read Full License

Additional Declarations: The authors declare no competing interests.

Aperture dilatation in DJAMILAR: Noether charge, localization drift, and a fixed-scale obstruction

Anisse Zerouta

Theoretical Physics Division, Precog Technologies, Paris, France
Corresponding author: a.zerouta@precogtec.com

September 2026

Abstract

In DJAMILAR the geometric state $\vartheta = \ln(C_d/C_{d,\mathrm{ref}})$, with $C_d = \pi n_d r_d^2$, enters a shift-symmetric scalar–aether gravitational sector, while the absolute aperture radius r_d also controls matter–memory couplings and a Gaussian localization channel. At fixed aperture density, the shift $\vartheta \to \vartheta + c$ is exactly the rescaling $r_d \to e^{c/2} r_d$. The purely shift-symmetric classical sector is therefore degenerate along the absolute aperture scale. On a homogeneous background, the dust-like temporal energy term is proportional to the Noether charge associated with this shift/dilatation orbit. For any strictly convex temporal function with minimum at $Q_0 > 0$, we prove a fixed-scale obstruction: if the comoving charge is nonnegative and the explicit breaking has the sign that produces positive charge, then $Q \geq Q_0$ and the aperture grows at least as $\exp[Q_0(t - t_i)/2]$. A strictly static aperture instead requires negative comoving charge, negative *temporal-sector* energy $-M_*^2 K(0)$, and an explicit breaking of the opposite sign. We derive the dilatation exponents of the localization and domain observables, including $M_c \propto r_d^{3(p+2-b_\gamma)/(3\alpha+p)}$, and identify normalization-free laboratory shape relations that are invariant under a common aperture drift. Assuming the positive-charge branch has held since a chosen initial epoch and imposing an ultraviolet floor gives $Q_0 \leq 2\ln(r_{d0}/\ell_{\mathrm{UV}})/(t_0 - t_i)$. For the benchmark $r_{d0} = 25$ nm this implies a present common drift below $4.5 \times 10^{-9}\,\mathrm{yr}^{-1}$ even for a Planck-length illustrative floor. In the separate tied-cutoff branch, where $G \propto r_d^2$, the solar-system bound $|\dot{G}/G| < 4 \times 10^{-14}\,\mathrm{yr}^{-1}$ strongly suppresses the allowed drift and, under the stated dark-remnant benchmark, requires $K_2 \gtrsim 8 \times 10^{16}$. The cosmological numbers are conditional; the shift/dilatation degeneracy and the fixed-scale obstruction are the model-level results.

Keywords: Djamilars; aperture dilatation; shift symmetry; Noether charge; ghost condensation; spontaneous localization; aether–scalar–tensor theory.

1 Introduction

The DJAMILAR programme assigns a geometric loading $C_d = \pi n_d r_d^2$ to a covariant scalar–aether sector and uses the associated aperture radius r_d in companion localization and matter–memory constructions [1, 2, 3, 4, 5]. The classical gravitational action belongs to the broader aether–scalar–tensor setting [6, 7, 8] and is shift symmetric in the scalar state ϑ. By contrast, the localization and domain sectors depend on the absolute value of ϑ through r_d. This mismatch creates a well-posed structural question: *can an absolute localization scale be dynamically stationary while the same homogeneous temporal sector carries a positive dust-like charge?*

The answer is conditional but sharp. At fixed proper aperture density, the constant shift of ϑ is not merely a field redefinition in the full construction: it rescales every aperture radius. The shift-symmetric classical sector is therefore exactly degenerate along an "aperture-dilatation" orbit, whereas the breaking sectors can measure position along that orbit. On an FLRW background the temporal current carries a conserved comoving charge when the breaking is absent; the dust-like term in the temporal energy density is proportional to that Noether charge near the charge-neutral condensate. The main theorem below shows that, for a strictly convex temporal function with minimum at $Q_0 > 0$, the positive-charge branch and a strictly fixed aperture are incompatible under the same sign of explicit breaking that generates the positive charge.

This statement is narrower than a no-go theorem for fixed localization scales in general. It applies to the assumptions listed in Sec. 2: the shift-symmetric classical representative, a

convex one-minimum temporal function, homogeneous evolution, and the common-state dictionary. A different breaking sign can approximately pin the aperture, but only by moving to the negative-charge branch and, in the temporal sector, negative energy relative to the charge-neutral condensate.
Five results follow, each stated with its level of proof.

1. **Aperture dilatation and scale degeneracy** (Section 3; DERIVED). At fixed n_d the shift $\vartheta \to \vartheta + c$ is the dilatation $r_d \to e^{c/2} r_d$. No observable computed from the shift-symmetric classical sector alone can determine the absolute r_d. If the induced Einstein coefficient is instead tied to r_d, current solar-system limits on $\dot{G}/G$ drive the benchmark temporal stiffness to $K_2 \gtrsim 8 \times 10^{16}$ (CONDITIONAL).

2. **Fixed-scale obstruction** (Section 4; DERIVED). For every strictly convex temporal function with minimum at $Q_0 > 0$, nonnegative comoving charge together with a positive-production breaking implies $Q \geq Q_0$; a static aperture requires negative charge, temporal-sector energy $-M_*^2 K(0)$ and a breaking force of the opposite sign. The temporal-sector energy is minimized at $Q = 0$, so the obstruction is dynamical/charge-theoretic rather than an energy barrier.

3. **Dilatation exponents** (Section 5; DERIVED). Breaking observables whose state dependence enters through r_d evolve along the homogeneous history with a computable logarithmic exponent. This unifies and generalizes the weakening law, the finite localization budget, the moving mass threshold and the past-injection factor of Ref. [5] to a state-dependent normalization $\gamma_{\rm loc} \propto r_d^{b_\gamma}$, and identifies the invariant laboratory ratios.

4. **A drift window from the laboratory aperture** (Section 6; DERIVED given stated premises, CONDITIONAL for the cosmological numbers). The present aperture and an ultraviolet floor bound the temporal chemical potential Q_0, hence the stiffness product $K_2 q_{s0}$.

5. **Tests and conditional targets** (Section 7). Laboratory co-drift and invariant-ratio tests, a conditional environment-transfer target, a solar-system exclusion of the tied-cutoff branch, and a relation between K_2 and the momentum-positivity scale of Ref. [5].

The paper does not predict the value of r_d, and it does not claim that the temporal remnant is the cosmological dark matter; where that identification is used, the result is labelled conditional. It does not assume that DJAMILAR is correct. It derives what the stated construction implies and what would falsify it. Status labels follow Ref. [5]: DERIVED (mathematical consequence of stated assumptions), CONDITIONAL (requires an identified extra premise), NUMERICAL (controlled computation), CONJECTURAL (motivated but not derived).

2 Minimal framework

2.1 Aperture state

The aperture variable is dimensionless,

$$\vartheta = \ln \frac{C_d}{C_{d,\rm ref}}, \qquad C_d = \pi n_d r_d^2, \tag{2.1}$$

where n_d is the proper aperture density and r_d the aperture radius [1, 2]. At fixed proper n_d,

$$r_d = r_{d,\rm ref}\, e^{\vartheta/2}. \tag{2.2}$$

Along the aether flow, $d\ln r_d/d\tau = Q/2$ with $Q = u^\mu \nabla_\mu \vartheta$ [2, 5]. Table 1 relates the notation of the five manuscripts.

Table 1: Notation used here and its origin. References: gravitation [2], quantum [3], reconstruction [4], memory [5], original preprint [1].

Quantity	Symbol here	Source and correspondence
aperture state	ϑ	all five; $\vartheta = \ln(C_d/C_{d,\mathrm{ref}})$
aperture radius, loading	r_d, C_d	[1, 2]; $r_d = r_{d,\mathrm{ref}} e^{\vartheta/2}$ at fixed n_d
temporal rate	$Q = u^\mu \nabla_\mu \vartheta$	[2, 5]
temporal function	$K(Q)$, K_2, Q_0	[2, 5]; $K = K_2(Q - Q_0)^2$
comoving temporal charge	$C_Q = a^3 K_Q$	[2, 5]
stiff-to-dust ratio	$q_s = C_Q/(4K_2 Q_0 a^3)$	[5]
memory field, mixing	Σ, $\bar\gamma$	[2] ($\bar\gamma$), [5] (γ)
domain effective mass	$\mu = M_d + U(\vartheta, \Sigma)$	[5]
localization rate	$\Gamma_D = \gamma_{\mathrm{loc}}(M/m_0)^\alpha F_p(R/r_d)$	[3, 4, 5]
normalization scaling	$\gamma_{\mathrm{loc}} \propto r_d^{\,b_\gamma}$	[5] (Sec. 4.4)

2.2 Classical sector and shift current

We use signature $(-,+,+,+)$ and $\hbar = c = 1$ unless stated. The classical sector is the scalar–aether–memory action of Refs. [2, 5],

$$S_{\mathrm{G}} = \frac{M_*^2}{2}\int d^4x\sqrt{-g}\,\Big[R - \tfrac{1}{2}K_B F_{\mu\nu}F^{\mu\nu} + 2Aa^\mu\nabla_\mu\vartheta - AY - AJ(Y;\Sigma) + 2K(Q) - \lambda(u^\mu u_\mu + 1)\Big] + \int d^4x\sqrt{-g}\,\Big[-\tfrac{1}{2}\nabla_\mu\Sigma\nabla^\mu\Sigma - V(\Sigma) - \bar\gamma\nabla_\mu\Sigma\,(a^\mu - u^\mu\Theta)\Big], \tag{2.3}$$

with $A = 2 - K_B$, $Y = D_\mu\vartheta D^\mu\vartheta$, $D_\mu\vartheta = h_\mu{}^\nu\nabla_\nu\vartheta$, $a^\mu = u^\nu\nabla_\nu u^\mu$ and $\Theta = \nabla_\mu u^\mu$. Ordinary matter ψ couples minimally to $g_{\mu\nu}$ through $S_M[\psi; g]$. The field ϑ appears in (2.3) only through $\nabla_\mu\vartheta$. The associated current

$$I^\mu = M_*^2\big[Aa^\mu - A(1 + J_Y)D^\mu\vartheta + K_Q u^\mu\big] \tag{2.4}$$

is conserved, $\nabla_\mu I^\mu = 0$, on solutions of $S_{\mathrm{G}} + S_M$ [2].

2.3 Breaking sectors

Three sectors depend on the absolute value of ϑ.

Domains. Rigid material domains of bare mass M_d carry the worldline action $-\sum_I \int \mu(\vartheta,\Sigma)\,d\tau_I$ with $\mu = M_d + U$ and, in the representative of Ref. [5], $U = E\Sigma^2 F(\vartheta)/f^2$, $F = 1/[1 + e^{\beta(\vartheta - \vartheta_R)}]$, $\beta = p/2$, $\vartheta_R = 2\ln(R/r_{d,\mathrm{ref}})$. The current then obeys $\nabla_\mu I^\mu = -nU_\vartheta$ [5].

Localization. A rigid domain of mass M and radius R undergoes Gaussian momentum transfers of width $\hbar/(\sqrt{2}r_d)$ at the rate [3, 4]

$$\Gamma_D = \gamma_{\mathrm{loc}}\Big(\frac{M}{m_0}\Big)^\alpha F_p\Big(\frac{R}{r_d}\Big), \qquad F_p(z) = \frac{z^p}{1 + z^p}, \qquad R_D(d) = \Gamma_D\big(1 - e^{-d^2/4r_d^2}\big). \tag{2.5}$$

Its momentum diffusion and heating are $D_C = \hbar^2\Gamma_D/(2r_d^2)$ per axis and $\dot E = 3\hbar^2\Gamma_D/(4Mr_d^2)$ [3]. We allow the bare normalization to scale as $\gamma_{\mathrm{loc}} \propto r_d^{\,b_\gamma}$ [5].

General homogeneous breaking. To keep the results independent of the microscopic origin of breaking, we also allow an arbitrary homogeneous breaking density $\mathcal{V}(\vartheta, t)$, of which $\mathcal{V} = nU$ is one case.

2.4 Assumptions

(A1) *Aperture dictionary:* Eqs. (2.1)–(2.2); fixed proper n_d where stated.

(A2) *Classical sector:* Eq. (2.3) with K, J, V, K_B, $\bar{\gamma}$ and M_*^2 independent of ϑ [2].

(A3) *Temporal function:* $K \in C^2$, $K'' > 0$, $K(Q_0) = K'(Q_0) = 0$ with $Q_0 > 0$. The quadratic representative is $K = K_2(Q - Q_0)^2$ [2, 5].

(A4) *Homogeneity:* spatially flat FLRW background with aligned aether, $a^\mu = 0$, $D_\mu \vartheta = 0$.

(A5) *Common state:* the laboratory aperture equals the homogeneous aperture at the same epoch, up to the environment corrections of Section 5.4 [5].

(A6) *Cosmological identification* (Section 6 only): the dust-like temporal term supplies the cold dark matter density Ω_c [9], production ended before recombination, and the stiff-to-dust ratio at $z_{\rm rec} \simeq 1100$ does not exceed 10^{-2}, a benchmark adopted in Ref. [5].

(A7) *Ultraviolet floor:* $r_d(t) \geq \ell_{\rm UV}$ over the interval $[t_i, t_0]$ in which the representative is used.

3 Aperture dilatation and scale degeneracy

3.1 The symmetry

Define the one-parameter family

$$\mathcal{D}_c : \qquad \vartheta \to \vartheta + c, \qquad (g_{\mu\nu}, u^\mu, \Sigma, \psi) \to (g_{\mu\nu}, u^\mu, \Sigma, \psi). \tag{3.1}$$

By (A1), $\mathcal{D}_c$ multiplies the loading by e^c and, at fixed n_d, every aperture radius by $e^{c/2}$. It is therefore a uniform dilatation of all apertures at fixed material content.

Proposition 1 (Gravitational blindness; DERIVED)**.** *Under (A1)–(A2), $S_{\rm G} + S_M$ is invariant under $\mathcal{D}_c$. If $(g, u, \vartheta, \Sigma, \psi)$ solves its field equations, so does $(g, u, \vartheta + c, \Sigma, \psi)$, with identical metric, aether, memory and matter histories. Every observable computed from $S_{\rm G} + S_M$ alone is independent of c, whereas $r_d \to e^{c/2} r_d$. Hence no such observable determines the absolute aperture radius. The radius enters observation only through (i) the domain coupling, (ii) the localization channel, or (iii) the stress–energy that these sectors inject into matter.*

Proof. Every ϑ-dependent term of (2.3) contains $\nabla_\mu \vartheta$, which is invariant under a constant shift, and S_M does not contain ϑ. The field equations are therefore invariant, and the solutions map onto one another with all other fields unchanged. □

Point (iii) matters in practice. Localization heating, $\dot{E} \propto \Gamma_D / r_d^2$, deposits energy into matter, which gravitates. Gravity is blind to r_d only at fixed matter energy.

3.2 The remnant is a Noether charge

On the homogeneous background (A4), $I^0 = M_*^2 K_Q$, and $\nabla_\mu I^\mu = -\partial_\vartheta \mathcal{V}$ becomes (Appendix A)

$$\dot{C}_Q = -\frac{a^3}{M_*^2}\, \partial_\vartheta \mathcal{V}, \qquad C_Q \equiv a^3 K_Q. \tag{3.2}$$

For $\mathcal{V} = nU$ with $n = n_0/a^3$ this is Eq. (11) of Ref. [5]. The temporal density and pressure are [2]

$$\rho_Q = M_*^2\,(Q K_Q - K), \qquad p_Q = M_*^2 K. \tag{3.3}$$

In the quadratic representative [5],

$$Q = Q_0 + \frac{C_Q}{2K_2 a^3}, \qquad \rho_Q = M_*^2 \Big(\frac{Q_0 C_Q}{a^3} + \frac{C_Q^2}{4K_2 a^6} \Big) = M_*^2 K_2 (Q^2 - Q_0^2). \tag{3.4}$$

The dust-like term $M_*^2 Q_0 C_Q/a^3$ is proportional to the Noether charge of the shift current, which becomes an aperture dilatation under the dictionary (2.2). Thus the temporal remnant is *carried by*, rather than identical to, this Noether charge. Its production in the domain representative [5] is explicit breaking of the shift/dilatation symmetry. For a general convex K with minimum at Q_0, the expansion of (3.3) about $K_Q = 0$ gives $\rho_Q = M_*^2 Q_0 C_Q/a^3 + O(C_Q^2/a^6)$, so the statement does not depend on the quadratic form. If $Q_0 = 0$, the leading term is $C_Q^2/(2K''(0)a^6)$ and no a^{-3} component exists.

3.3 The tied-cutoff branch

Proposition 1 assumes that M_*^2 does not depend on ϑ. In the induced-gravity interface of Ref. [2], $M_*^2 = \zeta_D \Lambda_D^2$ follows from the stress-trace correlator of a deep sector [10, 11], with its own correlation length ξ_D, not assumed equal to r_d. The alternative is worth quantifying.

Proposition 2 (Tied cutoff; CONDITIONAL)**.** *Suppose $\Lambda_D = \hbar c/(\lambda_D r_d)$ with constant λ_D and ζ_D. At fixed n_d the Newton coupling then scales as $G \propto r_d^2$, so that along the aether*

$$\frac{\dot{G}}{G} = 2\frac{\dot{r}_d}{r_d} = Q. \tag{3.5}$$

The coefficient required by the observed M_*^2 is $\zeta_D = \lambda_D^2 (r_d/\ell_P)^2/(8\pi) \simeq 9.5 \times 10^{52} \lambda_D^2$ for $r_d = 25$ nm. This is a dimensionless induced-gravity coefficient; it is not, by itself, a count of microscopic degrees of freedom.

With $Q \geq Q_0$ (Theorem 1 below), any local limit on a secular variation of Newton's constant becomes a direct limit on the tied branch. Lunar laser ranging gives $\dot{G}/G = (7.1 \pm 7.6) \times 10^{-14}\,\mathrm{yr}^{-1}$ [12], while the MESSENGER ephemeris analysis gives the tighter conditional solar-system bound $|\dot{G}/G| < 4 \times 10^{-14}\,\mathrm{yr}^{-1}$ after modeling the solar mass loss [13]. Using the latter gives $Q_0/H_0 \lesssim 5.8 \times 10^{-4}$. Combined with the remnant normalization of Section 6, this requires $K_2 q_{s0} \gtrsim 5.9 \times 10^5$, and $K_2 \gtrsim 7.9 \times 10^{16}$ if the stiff-ratio benchmark (A6) is imposed. The tied branch is therefore very strongly constrained. The untied construction of Ref. [2] avoids this direct $\dot{G}/G$ constraint because M_*^2 and r_d are independent scales.

4 The pinning–remnant exclusion

Theorem 1 (DERIVED)**.** *Assume (A2)–(A4) and a homogeneous breaking density $\mathcal{V}(\vartheta, t)$ entering Eq.* (3.2)*.*

(i) If $C_Q(t_i) \geq 0$ and $\partial_\vartheta \mathcal{V} \leq 0$ on $[t_i, t]$, then $Q \geq Q_0$ on $[t_i, t]$. The aperture state increases at least at the rate Q_0, and at fixed n_d the radius grows at least as $e^{Q_0(t-t_i)/2}$.

(ii) If $\bar{\vartheta}$ is constant on an open interval $\mathcal{I}$, then on $\mathcal{I}$

$$\begin{aligned} &Q = 0, \qquad K_Q = K'(0) < 0, \qquad C_Q = a^3 K'(0) < 0, \\ &\rho_Q = -M_*^2 K(0) < 0, \qquad \partial_\vartheta \mathcal{V} = 3M_*^2 H\,|K'(0)| > 0. \end{aligned} \tag{4.1}$$

(iii) Consequently, pinning is impossible for any breaking with $\partial_\vartheta \mathcal{V} \leq 0$, including the charge-producing domain coupling of Ref. [5]. For a breaking density without explicit time dependence, pinning requires H to be constant on $\mathcal{I}$.

(iv) For every strictly convex K, $d\rho_Q/dQ = M_*^2 Q K''(Q)$. On the temporal sector considered in isolation, ρ_Q is minimized at $Q = 0$, the static-aperture point.

Proof. (i) From (3.2), $\dot{C}_Q \geq 0$, hence $K_Q = C_Q/a^3 \geq 0$. Since K' is strictly increasing with $K'(Q_0) = 0$, $K_Q \geq 0$ is equivalent to $Q \geq Q_0$. (ii) A constant $\bar{\vartheta}$ means $Q = \dot{\bar{\vartheta}} = 0$. Convexity with minimum at $Q_0 > 0$ gives $K'(0) < 0$ and $K(0) > 0$. Equation (3.3) gives $\rho_Q = -M_*^2 K(0)$. Substituting $C_Q = a^3 K'(0)$ in (3.2) gives $3a^3 H K'(0) = -a^3 \partial_\vartheta \mathcal{V}/M_*^2$. (iii) The sign of $\partial_\vartheta \mathcal{V}$ in (4.1) is opposite to the hypothesis of (i). If $\mathcal{V}$ has no explicit time dependence, $\partial_\vartheta \mathcal{V}(\bar{\vartheta})$ is constant on $\mathcal{I}$, so H must be too. (iv) Differentiate (3.3): $d\rho_Q/dQ = M_*^2(K_Q + QK_{QQ} - K_Q) = M_*^2 Q K''$. □

Part (i) generalizes Eq. (22) of Ref. [5] from the quadratic representative and the domain coupling to every convex temporal function and every breaking of positive-production sign. Parts (ii)–(iv) are new.

Corollary 1 (Pinning–remnant fork; DERIVED)**.** *Within (A2)–(A4), a positive dust-like geometric remnant and an aperture held fixed over any interval with varying H cannot coexist. A dust-like term requires $Q_0 \neq 0$. For $Q_0 > 0$, a positive remnant forces $Q \geq Q_0$, while a static aperture forces $C_Q < 0$. For $Q_0 = 0$ a static aperture is allowed, but the temporal sector has no a^{-3} component.*

Item (iv) makes the result sharper than an energetic argument. The static-aperture point minimizes the temporal contribution ρ_Q, yet the positive-charge branch cannot reach it without changing the charge through a breaking of the opposite sign. The reason is charge conservation: in the absence of breaking, C_Q is conserved, $K_Q = C_Q/a^3 \to 0$, and $Q \to Q_0$ for any initial charge. Expansion drives the aperture towards the charge-neutral condensate $Q = Q_0$, which moves, not towards the energy minimum $Q = 0$, which does not. This is the symmetry-breaking pattern of ghost condensation [14]: the condensate $\dot{\bar{\vartheta}} = Q_0$ breaks time translations and the dilatation separately and preserves their diagonal combination. In DJAMILAR that combination has a physical reading. *A time translation of any localization experiment is equivalent to an aperture dilatation by $\int Q\, dt$.*

4.1 How close can an aperture come to being pinned?

A breaking with the anti-production sign can approximately pin the aperture. Take the quadratic representative and a restoring breaking $\mathcal{V} = M_*^2 K_2 \omega^2 (\vartheta - \vartheta_*)^2$ with constant ω. Equation (3.2) becomes

$$\dddot{\bar{\vartheta}} + 3H\ddot{\bar{\vartheta}} + \omega^2(\dot{\bar{\vartheta}} - \vartheta_*) = 3HQ_0. \tag{4.2}$$

Proposition 3 (Near-pinning; DERIVED, checked NUMERICALLY)**.** *For $\omega \gg H$, Eq. (4.2) has the adiabatic solution $\bar{\vartheta} = \vartheta_* + 3HQ_0/\omega^2 + O(H^3 Q_0/\omega^4)$, hence*

$$\frac{d\ln r_d}{dt} = \frac{3\dot{H}}{2}\frac{Q_0}{\omega^2}\Big[1 + O\Big(\frac{H^2}{\omega^2}\Big)\Big], \qquad \rho_Q = -M_*^2 K_2 Q_0^2\Big[1 + O\Big(\frac{H^4}{\omega^4}\Big)\Big], \qquad C_Q \simeq -2K_2 Q_0 a^3. \tag{4.3}$$

In the matter era the residual drift is $-\frac{9}{4}(H/\omega)^2 Q_0$. It vanishes only in an exactly de Sitter interval.

The derivation is given in Appendix B. Integrating (4.2) numerically with $H = 2/(3t)$ reproduces (4.3) to a relative accuracy better than 3×10^{-7} for $\omega t_i = 5$, 20 and 80 (Appendix D). Figure 1 compares the neutral condensate, a positive-production history and a near-pinned history. Near-pinning therefore places the temporal sector at a negative density $-M_*^2 K_2 Q_0^2$, which would have to be absorbed into the vacuum ledger of Ref. [2]; it continuously removes charge; and it leaves a residual drift fixed by $\dot{H}$.

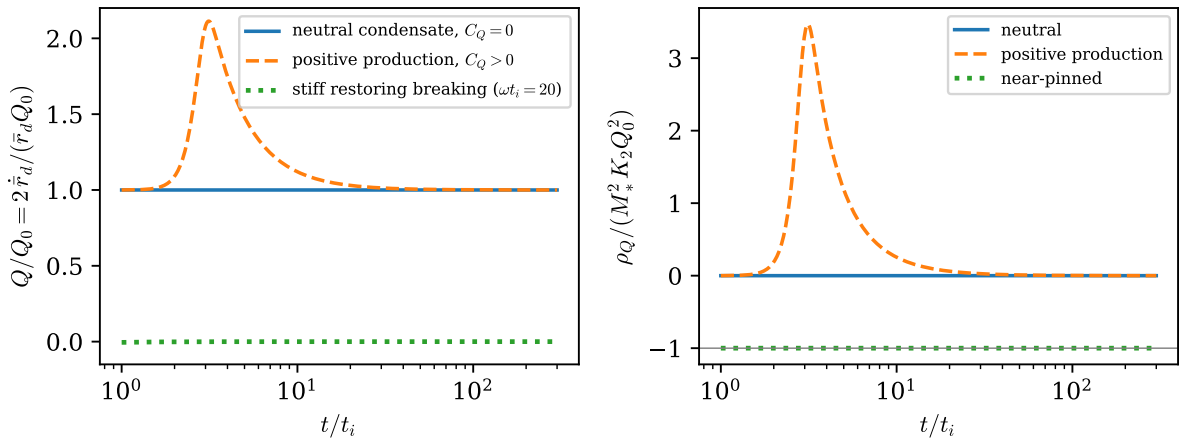


Figure 1: Homogeneous aperture histories in a matter-dominated background, quadratic representative with $K_2 = Q_0 = 1$ and t_i the initial time. Left: aperture rate $Q/Q_0 = 2\dot{\bar{r}}_d/(\bar{r}_d Q_0)$. Right: temporal energy density. Solid: neutral condensate, $C_Q = 0$. Dashed: charge produced by a breaking of positive-production sign; $Q \geq Q_0$ throughout, as required by Theorem 1(i). Dotted: restoring breaking with $\omega t_i = 20$; the aperture is nearly pinned, $\rho_Q \simeq -M_*^2 K_2 Q_0^2$ and the residual drift follows Eq. (4.3).

5 Dilatation exponents of breaking observables

5.1 General law

Let $O(r_d; \mathbf{m})$ be any observable produced by a breaking sector, evaluated at fixed material data $\mathbf{m} = (M, R, d, \dots)$. Define its dilatation exponent

$$\Delta_O \equiv \left.\frac{\partial \ln O}{\partial \ln r_d}\right|_{\mathbf{m}}. \tag{5.1}$$

Proposition 4 (DERIVED)**.** *Under (A1), (A4) and (A5), along the homogeneous history*

$$\frac{O(t_2)}{O(t_1)} = \exp\left[\frac{1}{2}\int_{t_1}^{t_2} \Delta_O\, Q\, dt\right]. \tag{5.2}$$

If $\Delta_O \to \Delta_\infty$ and the remaining prefactor approaches a finite nonzero limit while $Q \geq Q_0 > 0$, then $\Delta_\infty < 0$ guarantees exponential late-time decay and convergence of $\int^\infty O\, dt$, whereas $\Delta_\infty \geq 0$ does not. Over an interval on which Δ_O is constant, an accumulated winding $W = \int Q\, dt$ changes O by the exact factor $e^{\Delta_O W/2}$.

Proof. Equation (5.2) follows from $d\ln O/dt = \Delta_O\, d\ln r_d/dt$ and $d\ln r_d/dt = Q/2$. The remaining statements follow by direct integration, using $Q \geq Q_0$ for the convergence criterion. □

For the Hill law (2.5), Δ_O interpolates between the constant values in Table 2; the derivation is in Appendix C.

5.2 Consequences

Operational localization mass (DERIVED). For $R_c, d \ll r_d$, fixing $R_D T = \chi$ at constant density gives $R_c^{3\alpha+p} \propto r_d^{p+2-b_\gamma}$, so

$$M_c \propto r_d^{3(p+2-b_\gamma)/(3\alpha+p)}. \tag{5.3}$$

For $(\alpha, p, b_\gamma) = (1, 4, 0)$ this is the 18/7 law of Ref. [5]. A direct numerical solution of $R_D(R_c, r_d) =$ const agrees with (5.3) to better than 10^{-9} for five parameter sets (Appendix D). The threshold

Table 2: Dilatation exponents $\Delta_O = \partial \ln O / \partial \ln r_d$ at fixed material data, for the Hill activation (2.5) with $\gamma_{\rm loc} \propto r_d^{b_\gamma}$. "Closed" means $r_d \ll R, d$; "open" means $r_d \gg R, d$. For $b_\gamma = 0$ the open-aperture entries reproduce the weakening law and the 18/7 mass exponent of Ref. [5].

Observable	closed aperture	open aperture
event rate Γ_D	b_γ	$b_\gamma - p$
decoherence rate $R_D(d)$ at fixed d	b_γ	$b_\gamma - p - 2$
momentum diffusion D_C, heating $\dot{E}$	$b_\gamma - 2$	$b_\gamma - p - 2$
domain coupling $U \propto F$ (fixed Σ)	0	$-p$
production kernel $F(1-F)$	$+p$	$-p$
critical radius R_c at fixed attenuation	–	$(p + 2 - b_\gamma)/(3\alpha + p)$
operational mass $M_c \propto R_c^3$	–	$3(p + 2 - b_\gamma)/(3\alpha + p)$

is epoch-invariant only in the marginal case $b_\gamma = p + 2$, which is also the case of constant rate at fixed separation identified in Ref. [5].

Budget and past injection. Proposition 4 with the exponents of Table 2 reproduces the finite-budget conditions $b_\gamma < p$ (events) and $b_\gamma < p + 2$ (resolving action) of Ref. [5]. It generalizes the retrospective injection ratio of that paper to $e^{(p+2-b_\gamma)W/2}$ for open apertures.

Least-coupling rate (DERIVED). Along the positive-remnant history, the matter–aperture coupling of an open-aperture domain decays as $e^{-pQ_0 t/2}$ or faster. At the reference aperture it is already suppressed by $F(R/r_{d0})$: 2.0×10^{-11} for a Bohr-radius domain and 2.6×10^{-6} for a 1 nm domain ($p = 4$, $r_{d0} = 25$ nm). The couplings of macroscopic, saturated bodies do not decay; their fractional effect is instead suppressed by U/M_d.

5.3 Invariant laboratory ratios

Proposition 5 (Dilatation invariants; DERIVED under (A1), (A5))**.** *At fixed material data, every* intrinsic aperture length defined by a fixed value of a dimensionless crossover variable *is proportional to r_d. This includes the mechanically reconstructed aperture r_M of Ref. [4], the activation crossover radius $R_\times$ (where $F_p = 1/2$), and the separation crossover of Ref. [3]. Operational thresholds that also depend on exposure time, normalization or mass are not covered by this statement; their scaling is instead given by Proposition 4. Consequently:*

(a) their ratios, and all dimensionless shape data, are invariant in time and environment: p; α; the slope pair $3\alpha + p \to 3\alpha$ and its midpoint $3\alpha + p/2$; the null relation $\kappa = (S - 3\alpha)(3\alpha + p - S)$ [5]; the cumulant ratios $c_6 c_2 / c_4^2 = 5/3$ and $c_8 c_4 / c_6^2 = 7/5$, and $\eta = 1$ for a single aperture [4];

(b) any two aperture lengths ℓ_1, ℓ_2 drift together, $\ln[\ell_1(t_2)/\ell_1(t_1)] = \ln[\ell_2(t_2)/\ell_2(t_1)] = \frac{1}{2}\int_{t_1}^{t_2} Q\, dt$.

The invariants carry information about the breaking law; only dimensional aperture quantities carry information about ϑ.

5.4 Environment covariance

Spatial differences of ϑ are sourced by scalar gradients. The scalar-to-potential matching is not fixed in Ref. [2]. We write it as $\chi = \kappa_\chi c^2 \vartheta + \text{const}$, with κ_χ a dimensionless transfer coefficient that must be derived from the local matching problem.

Proposition 6 (CONDITIONAL on the matching)**.** *Between two static environments,*

$$\Delta \ln r_d = \frac{\Delta \chi}{2\kappa_\chi c^2}. \tag{5.4}$$

Table 3: Drift window for $r_{d0} = 25$ nm, $\Omega_c = 0.2642$, $H_0 = 2.184 \times 10^{-18}\,\mathrm{s}^{-1}$ and t_i at recombination. The three ℓ_{UV} rows use Eq. (6.1); the tied-cutoff row instead uses the MESSENGER bound $|\dot{G}/G| < 4 \times 10^{-14}\,\mathrm{yr}^{-1}$ [13]. The last column uses the loading $C_{d0} = 3.30 \times 10^{-8}$ of Ref. [1] and a contact loading $C_{\max} = \pi/4$ (Proposition 8).

ℓ_{UV}	$\ln(r_{d0}/\ell_{\mathrm{UV}})$	$Q_0/H_0 \le$	$K_2 q_{s0} \ge$	$K_2 \ge$ (A6)	drift today $\le$	$\tau_{\mathrm{c}} \ge$
Planck length	62.6	131.7	1.14×10^{-5}	1.5×10^{6}	$4.5 \times 10^{-9}\,\mathrm{yr}^{-1}$	1.9 Gyr
1 fm	17.0	35.8	1.54×10^{-4}	2.1×10^{7}	$1.2 \times 10^{-9}\,\mathrm{yr}^{-1}$	6.9 Gyr
Bohr radius	6.16	12.95	1.18×10^{-3}	1.6×10^{8}	$4.5 \times 10^{-10}\,\mathrm{yr}^{-1}$	19.2 Gyr
tied cutoff (Prop. 2)	–	5.80×10^{-4}	5.88×10^{5}	7.85×10^{16}	$2.0 \times 10^{-14}\,\mathrm{yr}^{-1}$	–

On a tracking branch with $\Delta\chi = \beta_0 \Delta\Phi_N$ [2], the Earth-surface-to-geostationary difference is $\Delta \ln r_d \simeq 3.0 \times 10^{-10} \beta_0/\kappa_\chi$, and the annual variation due to the orbital eccentricity is $1.6 \times 10^{-10}\beta_0/\kappa_\chi$ peak to peak. In a deep-MOND region, $\Delta\chi = v_f^2 \ln(r_2/r_1)$ gives $2.7 \times 10^{-7}/\kappa_\chi$ per e-fold of radius for $v_f = 220\ km\,s^{-1}$. An environment shift is equivalent to an epoch shift $\Delta t_{\mathrm{eq}} = \Delta\chi/(\kappa_\chi c^2 Q)$.

6 The drift window

Proposition 7 (Drift window; DERIVED given (A1), (A3), (A5), (A7) and $Q \ge Q_0$)**.** *If Theorem 1(i) holds on $[t_i, t_0]$, then*

$$Q_0 \le \frac{2\ln(r_{d0}/\ell_{\mathrm{UV}})}{t_0 - t_i}, \qquad \frac{d\ln r_d}{dt}\Big|_{t_0} = \frac{Q_0}{2}(1 + 2q_{s0}) \le \frac{(1 + 2q_{s0})\ln(r_{d0}/\ell_{\mathrm{UV}})}{t_0 - t_i}. \tag{6.1}$$

Proof. At fixed n_d, $\ln[r_{d0}/r_d(t_i)] = \frac{1}{2}\int_{t_i}^{t_0} Q\,dt \ge \frac{1}{2}Q_0(t_0 - t_i)$, and (A7) gives $\ln[r_{d0}/r_d(t_i)] \le \ln(r_{d0}/\ell_{\mathrm{UV}})$. The present rate follows from Eq. (3.4) with $q_{s0} = C_Q/(4K_2 Q_0 a_0^3)$. □

The bound uses only the present laboratory aperture, an ultraviolet floor and the age. It does not need the localization normalization, whose past value the retrospective argument of Ref. [5] would otherwise require.

Corollary 2 (Remnant stiffness; CONDITIONAL on (A6))**.** *With $\rho_c = 4M_*^2 K_2 Q_0^2 q_{s0}$ [5] identified with $3M_*^2 H_0^2 \Omega_c$,*

$$K_2 q_{s0} \ge \frac{3\Omega_c}{4}\left[\frac{H_0(t_0 - t_i)}{2\ln(r_{d0}/\ell_{\mathrm{UV}})}\right]^2. \tag{6.2}$$

The stiff-ratio benchmark $q_{s0} \le 10^{-2}/1101^3 = 7.49 \times 10^{-12}$ of (A6) then bounds K_2 from below.

We use the Planck base-ΛCDM values $h = 0.674$, $\Omega_c h^2 = 0.1200$, $t_0 = 13.797$ Gyr [9], and take t_i at recombination, so that $H_0(t_0 - t_i) = 0.951$. Table 3 gives the results for $r_{d0} = 25$ nm and three ultraviolet floors. The dependence on r_{d0} is only logarithmic: for $5 \le r_{d0} \le 50$ nm the Planck-floor bound on Q_0 changes by less than 3%. Figure 2 shows the allowed region in the $(K_2, Q_0/H_0)$ plane.

A lower bound on the present drift also follows from the remnant normalization, $d\ln r_d/dt|_{t_0} \ge Q_0/2 = (H_0/2)[3\Omega_c/(4K_2 q_{s0})]^{1/2}$. The present drift therefore lies in a window whose upper edge is fixed by the laboratory aperture and whose lower edge by the remnant stiffness.

Proposition 8 (Geometric saturation; DERIVED for any n_d history)**.** *Because $C_d = C_{d,\mathrm{ref}} e^{\vartheta}$ holds for every aperture-density history, $Q \ge Q_0 > 0$ implies that the loading reaches any fixed contact value $C_{\max}$ within*

$$\tau_{\mathrm{c}} \le \frac{\ln(C_{\max}/C_{d0})}{Q_0}. \tag{6.3}$$

If production has ended, Q decreases towards Q_0, and at fixed n_d Proposition 7 gives the lower bound $\tau_{\mathrm{c}} \ge \ln(C_{\max}/C_{d0})(t_0 - t_i)/[2(1 + 2q_{s0})\ln(r_{d0}/\ell_{\mathrm{UV}})]$.

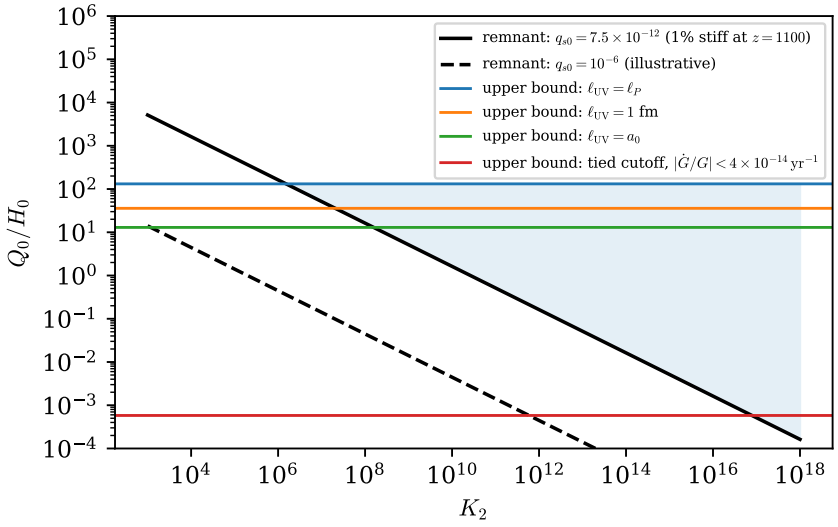


Figure 2: Drift window in the $(K_2, Q_0/H_0)$ plane. Black curves: remnant normalization $Q_0/H_0 = [3\Omega_c/(4K_2 q_{s0})]^{1/2}$ for the recombination stiff benchmark (solid) and an illustrative larger stiff ratio (dashed); a colder remnant lies above the curve. Horizontal lines: upper bounds (6.1) for three ultraviolet floors and the solar-system $\dot{G}/G$ bound of the tied-cutoff branch. The shaded region is allowed for the Planck floor and the benchmark stiff ratio.

Unlike the radius, the loading cannot be held fixed by any evolution of the aperture density. With the geometry of the original proposal [1] ($\ell = 244\ \mu$m, $r_d = 25$ nm), $\ln(C_{\rm max}/C_{d0}) = 17.0$ for square contact ($\pi/4$) and 17.1 for hexagonal contact ($\pi/2\sqrt{3}$). If production has ended and the benchmark history is extrapolated without new breaking, the contact time is bounded below by 1.9 Gyr for the illustrative Planck-length floor (Table 3); this is not a prediction that the effective theory remains valid to contact. What happens at contact is not described by the present effective theory.

7 Tests

T1 — Laboratory invariants and co-drift. The reconstruction programme of Refs. [3, 4] measures r_M, $R_\times$, the separation crossover and the dimensionless data of Proposition 5. The common-state realization predicts that the intrinsic aperture-length ratios remain constant between campaigns. Under the additional history and ultraviolet-floor premises of Proposition 7, the common drift is bounded by $4.5 \times 10^{-9}\,{\rm yr}^{-1}$ for the illustrative Planck floor. Relative drift between two intrinsic aperture lengths would falsify the common-state identification directly; exceeding the absolute drift bound would instead falsify the full set of assumptions entering Proposition 7.

T2 — Environment-transfer target. Repeating an aperture reconstruction on the ground and in orbit would probe Eq. (5.4). For $|\beta_0/\kappa_\chi| \sim 1$, the Earth-surface-to-geostationary estimate is of order 3×10^{-10} in $\Delta \ln r_d$. Because κ_χ has not yet been derived, this is a conditional target rather than a parameter-independent null test.

T3 — Solar-system ranging and the tied cutoff. Equation (3.5) converts every local $\dot{G}/G$ bound into a bound on Q. The MESSENGER limit $|\dot{G}/G| < 4 \times 10^{-14}\,{\rm yr}^{-1}$ [13], together with the benchmark remnant identification, gives $K_2 \gtrsim 7.9 \times 10^{16}$ in the tied branch (Table 3).

T4 — Stiffness and the momentum-positivity scale. Under its matching assumptions, Ref. [5] gives the present momentum-positivity wavenumber $q^2_{\mathrm{kin},0} \simeq (9/8)\Omega_b\Omega_c H_0^2/q_{s0}$. Corollary 2 implies $q_{s0} \geq X/K_2$ with $X = 1.14 \times 10^{-5}$ at the Planck floor, hence

$$\lambda_{\mathrm{kin},0} = \frac{2\pi}{q_{\mathrm{kin},0}} \geq \frac{780\ \mathrm{Mpc}}{\sqrt{K_2}} \qquad (\Omega_b = 0.0492,\ \Omega_c = 0.2642). \tag{7.1}$$

The boundary can fall below the 0.63 Mpc of Ref. [5] only if $K_2 \gtrsim 1.5 \times 10^6$, which is the Planck-floor entry of Table 3. The two results are mutually consistent. They make the momentum-positivity question of Ref. [5] and the value of K_2 a single problem.

T5 — Thermal history. If a lower bound on the past normalization becomes available, the injection into diffuse neutral gas scales as $e^{(p+2-b_\gamma)W/2}$ (Table 2), with $W \leq 2\ln(r_{d0}/\ell_{\mathrm{UV}})$ by Proposition 7. The thermal and ionization history then bounds the combination $(p+2-b_\gamma)W$.

8 Comparison with known constructions

Ghost condensation and AeST. The condensate $\dot{\vartheta} = Q_0$ and its symmetry-breaking pattern are those of ghost condensation [14]. The dust-like behaviour of a shift charge near Q_0 is the AeST mechanism [6, 7, 8]. In those theories the absolute scalar zero mode is not itself assigned the localization-length meaning used here. Proposition 1 is therefore a symmetry statement already familiar in spirit, whereas its aperture interpretation and the fixed-scale obstruction acquire observable content only after the DJAMILAR dictionary and breaking sectors are imposed.

Dilatonic condensates. Piazza and Tsujikawa studied a ghost condensate whose field is a dilaton [15]. There the dilaton dependence multiplies the kinetic function, so the symmetry is broken in the gravitational sector itself. Here the gravitational sector is exactly shift symmetric, and the dilaton meaning comes only from the breaking sectors. The tied-cutoff branch of Proposition 2 is the closest analogue, and lunar ranging disfavours it.

Affleck–Dine mechanism. Charge generation by explicit breaking while a field evolves, followed by conservation once the breaking switches off, is the structure of the Affleck–Dine mechanism [16]. In its Nambu–Goldstone form, the charge is carried by the angular motion of a Goldstone field [17]. The correspondence with Ref. [5] is structural: rotation corresponds to the winding $\dot{\vartheta}$, the explicit breaking to nU, and the switch-off to $F \to 0$. Two differences are quantitative. The breaking sign is fixed by positivity of production (Theorem 1(i)). And the switch-off is enforced by the winding itself, at the rate $e^{-pQ_0t/2}$ of Table 2. A shift-symmetric charge can also be generated through a curvature coupling [18], which parallels the curvature-driven memory of Ref. [5].

Runaway dilaton and least coupling. In the least-coupling and runaway-dilaton scenarios, matter couplings vanish as the field runs to a decoupling limit [19, 20]. Here the runaway is not produced by a potential. It is forced by the sign of the remnant, and the coupling of an open-aperture domain vanishes as $(R/r_d)^p$. Field-dependent masses of matter have a longer history [21, 22, 23], and the domain coupling of Ref. [5] belongs to that class. The new element is its activation by the ratio of two lengths, which ties the decay rate of the coupling to the localization exponent p.

9 Limitations

- The analysis is classical and homogeneous. Whether quantum corrections generate a breaking with the anti-production sign, the only way to approach pinning (Proposition 3), is not addressed. A radiatively selected aperture scale therefore remains open, but Corollary 1 states what it would cost.

- The convex class (A3) is assumed. Temporal functions with several minima are not covered.

- Fixed aperture density is used for the radius results. If n_d evolves, the radius can stay fixed while ϑ winds, but the loading cannot (Proposition 8).
- The common-state assumption (A5) and the scalar matching coefficient κ_χ are not derived. Consequently, the environment estimates are conditional targets rather than current parameter-free predictions.
- The cosmological numbers depend on (A6), including production before recombination and the one-percent stiff benchmark, and on the choice of $\ell_{\rm UV}$. The Planck length is used only as an illustrative extreme floor; no validity of the effective description down to the Planck scale is assumed. The product bound (6.2) does not use the one-percent benchmark, but it still requires the remnant-density identification.
- The normalization exponent b_γ is unknown. All exponent statements are given as functions of it.
- The localization channel is a prescribed test channel, without backreaction, as in Refs. [3, 5].

10 Conclusion

At fixed aperture density, the shift orbit of the DJAMILAR scalar is an aperture-dilatation orbit. The shift-symmetric classical sector cannot determine where the system sits on that orbit; only the explicit breaking sectors can give the absolute aperture scale operational meaning. On homogeneous backgrounds, the dust-like temporal energy is proportional to the associated Noether charge near the charge-neutral condensate.

The main result is the fixed-scale obstruction. Within the strictly convex one-minimum class, nonnegative comoving charge together with the positive-production sign implies $Q \geq Q_0 > 0$ and therefore secular aperture growth. A strictly static aperture lies instead on the negative-charge branch and requires a breaking of the opposite sign. The temporal-sector energy is minimized at the static point, so the obstruction is not an energy barrier but a consequence of the charge branch and its balance law. The same dilatation structure organizes the scaling of localization observables, separates true common-aperture invariants from protocol-dependent thresholds, and turns an assumed ultraviolet floor into a conditional bound on the temporal clock.

The quantitative cosmological bounds remain model dependent: they require the common-state dictionary, a specified history, an ultraviolet floor and, where used, identification of the temporal remnant with the dark-matter density. The tied-cutoff branch is additionally subject to strong solar-system limits on $\dot{G}/G$. The robust content is therefore narrower than a generic no-go theorem: *within the stated DJAMILAR representative and sign choice, a positive dust-like charge and a strictly fixed common localization aperture cannot coexist.* Any microscopic completion that seeks both must alter at least one of those premises.

A Homogeneous Noether balance

With a breaking density $\mathcal{V}(\vartheta, t)$ added to the action as $-\int \sqrt{-g}\,\mathcal{V}$, variation with respect to ϑ gives $\nabla_\mu I^\mu = -\partial_\vartheta \mathcal{V}$. On (A4), $a^\mu = 0$ and $D^\mu \vartheta = 0$, so $I^\mu = M_*^2 K_Q u^\mu$ and $\nabla_\mu I^\mu = a^{-3}\, d(a^3 M_*^2 K_Q)/dt$. This gives Eq. (3.2). For domains, $\mathcal{V} = nU$ reproduces $\dot{C}_Q = -(n_0/M_*^2)U_\vartheta$ [5].

B Near-pinning expansion

Write $\bar{\vartheta} = \vartheta_* + x$ in Eq. (4.2): $x = (3HQ_0 - 3H\dot{x} - \ddot{x})/\omega^2$. Iterating, $x_0 = 3HQ_0/\omega^2$, $\dot{x}_0 = 3\dot{H}Q_0/\omega^2$, and the next correction is $-(9H\dot{H} + 3\ddot{H})Q_0/\omega^4$, of relative order H^2/ω^2. Then $Q = \dot{x}$ and $\rho_Q = M_*^2 K_2(\dot{x}^2 - Q_0^2) = -M_*^2 K_2 Q_0^2[1 - O(H^4/\omega^4)]$. The breaking energy is $\mathcal{V} = M_*^2 K_2 \omega^2 x^2 \simeq$

$9M_*^2K_2H^2Q_0^2/\omega^2$. The charge is $C_Q = 2K_2a^3(\dot{x} - Q_0) \simeq -2K_2Q_0a^3$, which the breaking must remove at the rate $6K_2Q_0Ha^3$.

C Dilatation exponents of the Hill law

With $z = R/r_d$, $\partial \ln F_p/\partial \ln r_d = -p(1 - F_p)$, which tends to $-p$ for $z \to 0$ and to 0 for $z \to \infty$. With $\xi = d^2/4r_d^2$, $\partial \ln(1 - e^{-\xi})/\partial \ln r_d = -2\xi/(e^\xi - 1)$, which tends to -2 for $\xi \to 0$ and to 0 for $\xi \to \infty$. For $F(1 - F)$, the exponent is $-p(1 - F) + pF = p(2F - 1)$, from $+p$ to $-p$. Momentum diffusion and heating carry an extra r_d^{-2}. For the critical radius, $\ln R_D = b_\gamma \ln r_d + 3\alpha \ln R + \ln F_p + \ln(1 - e^{-\xi}) + \text{const}$, and $d \ln R_D = 0$ at fixed d gives $d \ln R_c/d \ln r_d = [p(1 - F) + 2\xi/(e^\xi - 1) - b_\gamma]/[3\alpha + p(1 - F)] \to (p + 2 - b_\gamma)/(3\alpha + p)$ for $R_c, d \ll r_d$.

D Numerical verification

The script `verify_dilatation.py`, supplied with the manuscript, checks: (a) $\rho_Q(0) = -M_*^2K_2Q_0^2$ and the minimum of ρ_Q at $Q = 0$; (b) $\min_t(Q - Q_0) = 0$ for a positive-production history, i.e. $Q \geq Q_0$ throughout; (c) the near-pinning law (4.3), with maximal relative deviations 9.7×10^{-10}, 1.5×10^{-8} and 2.3×10^{-7} for $\omega t_i = 5$, 20 and 80; (d) the mass exponent (5.3) for $(\alpha, p, b_\gamma) = (1, 4, 0)$, $(1, 4, 2)$, $(1, 4, 6)$, $(1, 2, 0)$ and $(2, 4, 0)$, with numerical values 2.5714, 1.7143, 0.0000, 2.4000 and 1.8000; (e) all entries of Table 3 and the environment estimates of Proposition 6. The figure script `figures.py` regenerates Figs. 1 and 2.

Declarations

Funding. This research received no external funding.
Competing interests. The author declares no competing interests. The affiliation with Precog Technologies is provided as a professional affiliation; Precog Technologies did not fund, sponsor or commission the work reported in this manuscript.
Data availability. No new observational or experimental data set was generated. The verification and figure scripts are supplied as supplementary material. Published cosmological and solar-system ranging values are taken from the cited literature.

References

[1] A. Zerouta, "Gravity as geometric filtration: A unified framework for cosmological and quantum phenomena," Research Square preprint, version 1 (2025). doi:10.21203/rs.3.rs-6570489/v1.

[2] A. Zerouta, "DJAMILAR: Gravity as geometric filtration—a common geometric origin of gravitation, quantum–classical behaviour and dark-sector phenomenology," Research Square preprint, version 1 (2026). doi:10.21203/rs.3.rs-11144964/v1.

[3] A. Zerouta, "Djamilar-induced localization and the quantum–classical transition," Research Square preprint, version 1 (2026). doi:10.21203/rs.3.rs-11162349/v1.

[4] A. Zerouta, "DJAMILAR: Reconstructing the geometry of the quantum–classical transition—a common-aperture test linking matter-wave coherence and mechanical fluctuations," Research Square preprint, version 1 (2026). doi:10.21203/rs.3.rs-11189947/v1.

[5] A. Zerouta, "DJAMILAR: Geometric charge and the evolution of localization—memory, cosmological transport and a finite localization budget," manuscript (2026).

[6] C. Skordis and T. Zlosnik, "New relativistic theory for Modified Newtonian Dynamics," Phys. Rev. Lett. **127**, 161302 (2021). doi:10.1103/PhysRevLett.127.161302.

[7] C. Skordis and T. Zlosnik, "Aether scalar tensor theory: Linear stability on Minkowski space," Phys. Rev. D **106**, 104041 (2022). doi:10.1103/PhysRevD.106.104041.

[8] M. Bataki, C. Skordis and T. Zlosnik, "Aether scalar tensor theory: Hamiltonian formalism," Phys. Rev. D **110**, 044015 (2024). doi:10.1103/PhysRevD.110.044015.

[9] Planck Collaboration, "Planck 2018 results. VI. Cosmological parameters," Astron. Astrophys. **641**, A6 (2020). doi:10.1051/0004-6361/201833910.

[10] S. L. Adler, "A formula for the induced gravitational constant," Phys. Lett. B **95**, 241 (1980).

[11] A. Zee, "Spontaneously generated gravity," Phys. Rev. D **23**, 858 (1981).

[12] F. Hofmann and J. Müller, "Relativistic tests with lunar laser ranging," Class. Quantum Grav. **35**, 035015 (2018). doi:10.1088/1361-6382/aa8f7a.

[13] A. Genova, E. Mazarico, S. Goossens et al., "Solar system expansion and strong equivalence principle as seen by the NASA MESSENGER mission," Nat. Commun. **9**, 289 (2018). doi:10.1038/s41467-017-02558-1.

[14] N. Arkani-Hamed, H.-C. Cheng, M. A. Luty and S. Mukohyama, "Ghost condensation and a consistent infrared modification of gravity," JHEP **05**, 074 (2004). doi:10.1088/1126-6708/2004/05/074.

[15] F. Piazza and S. Tsujikawa, "Dilatonic ghost condensate as dark energy," JCAP **07**, 004 (2004). arXiv:hep-th/0405054.

[16] I. Affleck and M. Dine, "A new mechanism for baryogenesis," Nucl. Phys. B **249**, 361 (1985). doi:10.1016/0550-3213(85)90021-5.

[17] K. Harigaya, "Nambu–Goldstone Affleck–Dine baryogenesis," JHEP **08**, 085 (2019). doi:10.1007/JHEP08(2019)085.

[18] A. De Simone, T. Kobayashi and S. Liberati, "Geometric baryogenesis from shift symmetry," Phys. Rev. Lett. **118**, 131101 (2017). arXiv:1612.04824.

[19] T. Damour and A. M. Polyakov, "The string dilaton and a least coupling principle," Nucl. Phys. B **423**, 532 (1994). doi:10.1016/0550-3213(94)90143-0.

[20] T. Damour, F. Piazza and G. Veneziano, "Runaway dilaton and equivalence principle violations," Phys. Rev. Lett. **89**, 081601 (2002). doi:10.1103/PhysRevLett.89.081601.

[21] T. Damour, G. W. Gibbons and C. Gundlach, "Dark matter, time-varying G, and a dilaton field," Phys. Rev. Lett. **64**, 123 (1990). doi:10.1103/PhysRevLett.64.123.

[22] G. W. Anderson and S. M. Carroll, "Dark matter with time-dependent mass," arXiv:astro-ph/9711288 (1997).

[23] L. Amendola, "Coupled quintessence," Phys. Rev. D **62**, 043511 (2000). doi:10.1103/PhysRevD.62.043511.